Phase error corrected 4-bit true time delay module using a cascaded 2 × 2 polymer waveguide switch array

Xiaolong Wang, Brie Howley, Maggie Y. Chen, and Ray T. Chen

A fully integrated 4-bit true time delay device using polymer optical switches and waveguide delay lines is demonstrated. The fabricated device, which contains five 2 × 2 thermo-optic switches, has a maximum power consumption of 143 mW and a switching time less than 3 ms. The rf phase error, which is affected by the optical switch cross talk, is also theoretically analyzed and proved to be negligible by experimental results. © 2007 Optical Society of America

OCIS codes: 130.0130, 060.1810, 130.3120.

1. Introduction

Optical true time delay (TTD) for phased-array antennas offers many advantages over electrical phase delays such as wide bandwidth, immunity to electromagnetic interference, and compact size.[1] Compared with the wavelength tuning configuration,[2] an optically switched waveguide delay line device structure[3] needs no tunable wavelength sources, resulting in reduced system costs and enhanced resistance to harsh environments. Another delay device structure composed of optical microelectromechanical system (MEMS) switches and fiber delay lines[4] shows desirable features such as low insertion loss. A novel design based on MEMS and free-space white cell[5] also shows potential in terms of speed and scalability. However, either the fiber length has to be precisely cut or the mirrors have to be exactly assembled to achieve accurate delays.

A more attractive approach is to integrate waveguide switches and delay lines on a single chip by the planar lightwave circuit technique. A previously reported 2-bit TTD configuration using polymer optical switches and waveguide delay lines,[5] which are defined by photolithography, can precisely deliver four TTDs. The fully integrated photonic circuit eliminates the discrete between optical switches and fibers; therefore, it provides a more stable throughput and occupies less space. Additionally, the fabrication cost is significantly reduced. In this paper, we present an implementation of a 4-bit polymer TTD device containing five fully integrated 2 × 2 thermo-optic switches based on the total internal reflection (TIR) effect. Compared with other optical switch structures, such as Mach–Zenhder interferometers[6] or directional couplers,[7] TIR switches have a much lower cross talk,[8] which significantly decreases the rf signal phase error. Additionally, the switching operation of TIR switches is not sensitive to the wavelength, thus providing a large optical bandwidth. Compared with digital optical switches,[9] TIR switches are more compact, with lengths of only several millimeters and require lower driving powers.

2. Design, Fabrication, and Experimental Results

The configuration of the proposed TTD device is shown in Fig. 1(a). The device is composed of input–output waveguides, five 2 × 2 TIR thermo-optic switches, four reference lines, and four delay lines, which give 16(2^4) delay combinations. Both optical switches and waveguide delay lines have a core index of 1.46 and a cladding index of 1.45. The 6.5 μm × 6.5 μm channel waveguide cross section constrains the waveguide to the single-mode condition and provides a measured coupling efficiency of 85% with a single-mode fiber. The TIR switches have a 250 μm waveguide separation and a 4° half-branch angle, as seen in Fig. 1(b). For each crossing region, the waveguides are tapered from 6.5 to 48 μm to reduce the cross talk.[10] The switches are 4924 μm in length including 500 μm straight waveguide segments on each side to stabilize the optical mode into and out of the delay lines. Microheaters are placed on the top

The authors are with the Microelectronics Research Center, University of Texas at Austin, Austin, Texas 78758. R. T. Chen's e-mail address is chen@ece.utexas.edu.

Received 19 April 2006; revised 10 July 2006; accepted 18 July 2006; posted 19 September 2006 (Doc. ID 70106); published 4 January 2007.

0003-6935/07/030379-05$15.00/0

© 2007 Optical Society of America

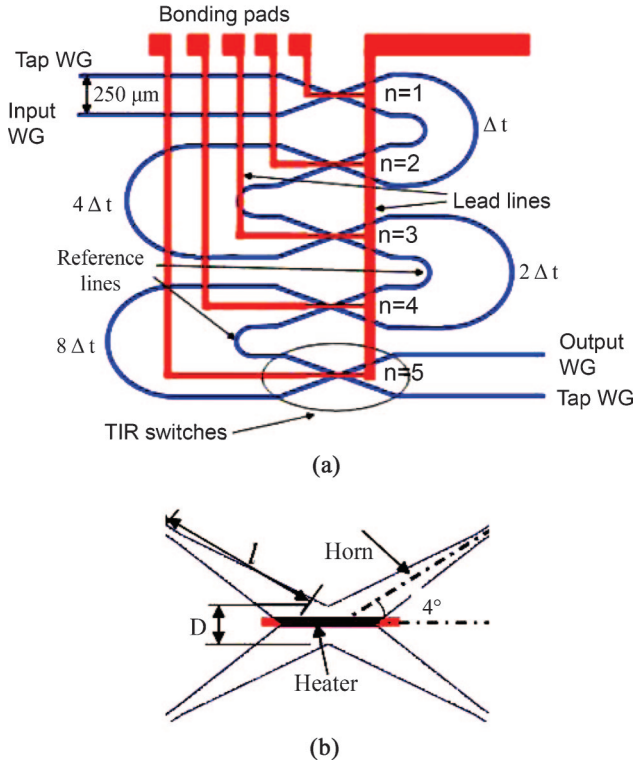

Fig. 1. (Color online) (a) Schematic of the 4-bit TTD device using TIR optical switches. (b) Schematic of the TIR optical switches.

cladding layer and are connected to bonding pads through lead lines. The bend radii of the reference lines are 1.5 mm, and those of the delay lines are 1.75 mm. The proposed 4-bit TTD device can dynamically deliver 16 delays from 0 to 177 ps with 11.8 ps increments, which are determined by the lengths of the waveguide delay lines.

UV curable fluorinated acrylates, ZPU12-460 and ZPU12-450 from ChemOptics, are used as the core and cladding materials. They are spin coated and etched by reactive ion etching to form the waveguide structure. The microheaters and lead lines, including bonding pads, are patterned by a lift-off process to obtain a uniform linewidth. In the backend process, the TTD device is diced and polished to obtain good coupling facets with single-mode fibers. Figure 2 shows the fabricated 4-bit TTD device with an enlarged view of the TIR thermo-optic switch. The chip die dimension is 21.7 mm × 13.7 mm.

To route the optical signal to a single output waveguide, zero, two, or four switches are required to be activated. The working states of the five switches, as well as the total power consumption, in the 16 delay configurations are shown Table 1. The maximum power consumption is 143 mW when four switches are fully activated. The average operating power of a single TIR switch is only $\frac{1}{10}$ of that required for a digital optical switch. The switching speed of the TIR switches is measured by applying a 50 Hz square wave signal with a 50% duty cycle. Both the on and off state switching times are measured to be less than 3 ms, as shown in Fig. 3.

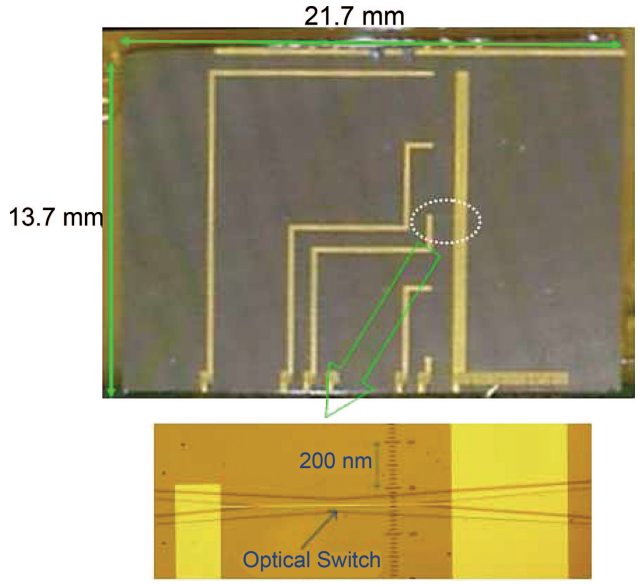

Fig. 2. (Color online) Chip die of the 4-bit TTD device with an enlarged view of the optical switch.

3. Radio Frequency Performance

The rf performance, namely, the rf phase error caused by the optical switch cross talk, is analyzed in this section. Two typical structures are presented to be compared with each other. Figure 4(a) uses a 2 × 1 combiner as the output waveguide, which is described in Refs. 11 and 12 while Fig. 4(b) uses a 2 × 2 switch, corresponding to the structure in this paper. The analysis procedure, from Eq. (1) to Eq. (6), follows the work done in Ref. 11.

We assume the cross-talk values as CT for all the five switches both in the cross and bar states and neglect the propagation loss of delay lines for simplicity. For each switch, the splitting ratio of the optical E field is

$$a{:}b = \sqrt{10^{(\mathrm{CT}/10)}}{:}1. \tag{1}$$

The minor signals from each switch will travel through undesired paths. Some of these signals will be transferred to the redundant waveguide, which is not harmful to the output signal quality. However, some of these signals will be routed to the output waveguide, which will cause a rf signal phase error. For analysis, we assume all 16 possible delays will be routed to the output waveguide, so the optical E field at the detector is

$$E = E_0 e^{j\omega}\left(C_1 e^{j\phi_1} + C_2 e^{j\phi_2} + \cdots + C_{16} e^{j\phi_{16}}\right). \tag{2}$$

E_0 is the normalized field amplitude, ω is the optical angular velocity, C_i is the coefficient of the ith delay, and ϕ_i is the rf phase delay. Neglecting the optical angular frequency, which is much higher than the rf signals, the intensity of the optical signal that will be detected is

Table 1. Delay Configuration, Power Consumption, and RF Performance

Time Delay (Δt)	Switches Activated	Driving Power (mW)	Calculated Phase Error at 10.5 GHz (deg)	Measured Phase Standard Deviation (deg)	Delay Error (ps)
0	1,5	67	−0.04	0.94	−0.022
1	2,5	66	−0.14	0.39	0.221
2	1,3,4,5	137	0.08	0.43	0.504
3	2,3,4,5	137	0.12	0.35	0.236
4	1,2,3,5	141	0.02	0.67	0.227
5	3,5	66	0.14	0.61	0.086
6	1,2,4,5	141	0.08	0.75	−0.745
7	4,5	65	0.08	0.76	−0.383
8	1,4	68	−0.04	0.57	0.379
9	2,4	67	−0.14	0.64	−0.351
10	1,3	68	−0.15	0.68	−0.197
11	2,3	68	−0.08	0.57	−0.415
12	1,2,3,4	143	−0.02	0.48	−0.418
13	3,4	67	0.14	0.55	0.175
14	1,2	70	0.16	1.14	−0.446
15	None	0	0.19	1.08	−0.008

$$I = E_0\left(C_1 e^{j\phi_1} + C_2 e^{j\phi_2} + \cdots + C_{16} e^{j\phi_{16}}\right) \times E_0\left(C_1 e^{j\phi_1} + C_2 e^{j\phi_2} + \cdots + C_{16} e^{j\phi_{16}}\right). \quad (3)$$

By expanding Eq. (3) into the sum of polynomials, each ith detected rf envelope signal has the coefficient of

$$X_i = \sum_{j=1}^{16} C_i C_j \cos(\phi_i - \phi_j). \quad (4)$$

For example, X_1 is the desired signal, while the undesired signals, $X_2, X_3, \ldots, X_{16}$ will function as noise. Combining all the rf signals as Fig. 5 shows, the measured rf signal X_1' has a phase error with respect to X_1,

$$\phi_{\text{error},i} = \tan^{-1} \frac{\sum_{j=1, j\neq i}^{16} X_j \sin(\phi_j - \phi_i)}{X_i + \sum_{j=1, j\neq i}^{16} X_j \cos(\phi_j - \phi_i)}. \quad (5)$$

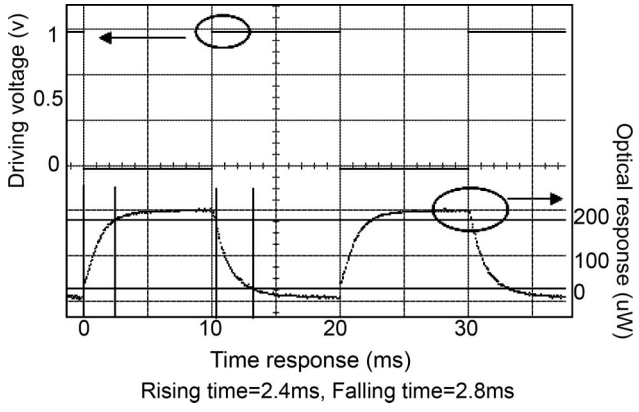

Fig. 3. Switching speed measurement of the 4-bit TTD device.

In Fig. 4(a), the first-order minor signals (E-field splitting ratios are a:b), which go through one switch's undesired port, will leak through the redundant output waveguide. Only second-order minor signals (E-field splitting ratios are a^2:b^2), which go through two switches' undesired ports, have the opportunity to be detected, and totally there are $C_5^2 = 10$ possible signals. Based on Eq. (1), which provides the E-field splitting ratios between the major and minor ports, the phase error caused by the second-order minor signals is

$$\phi_{\text{error},i} = \tan^{-1} \frac{b^2 \sum_{j=1}^{10} \sin(\phi_j - \phi_i)}{a^2 + b^2 \sum_{j=1}^{10} X_j \cos(\phi_j - \phi_i)}. \quad (6)$$

In the 2 × 1 combiner structure shown in Fig. 4(b), all first-order minor signals, which are the main noise contributors, plus higher-order minor signals, will be captured. The phase error can vary with different delay configurations, depending on the working states of the optical switches. Figure 6 shows the simulated results of the rf phase error due to the cross talk for the delay value of $15\Delta t$ when the rf is 10.5 GHz. The 2 × 2 switch TTD

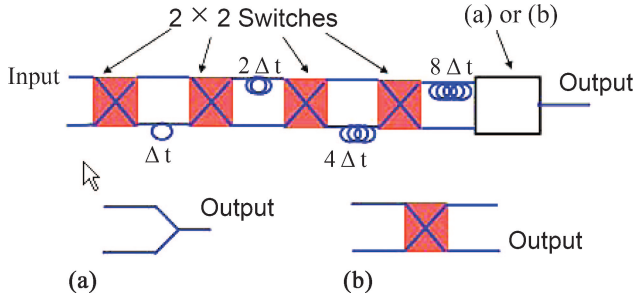

Fig. 4. (Color online) Four-bit TTD device, the last stage using (a) 2 × 1 combiner, (b) 2 × 2 optical switch.

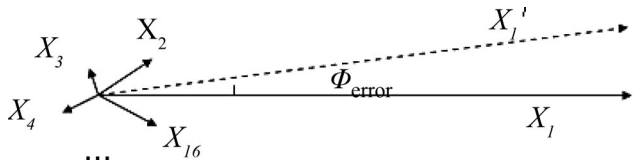

Fig. 5. Illustration of the rf signal phase error in the 4-bit TTD device.

device structure has a smaller phase error than that of the 2×1 combiner one. But even with the 2×2 switch structure, -20 dB cross talk still causes a 2° phase error. To overcome the volume-relaxation-induced cross-talk aggravation of polymer TIR switches, a large half-branch angle of 4° is chosen since it can offer a dynamic cross talk below -30 dB.[8] All possible rf phase errors due to the cross talk are simulated and shown in Table 1.

To experimentally evaluate the impact of the optical switch cross talk upon the rf signal phase error, we measured the phase error from 6 to 12 GHz when the delay is $15\Delta t$ shown in Fig. 7. A HP8510C network analyzer, which provided a continuously scanning microwave from 6 to 12 GHz, drove a 40 GHz $LiNbO_3$ modulator to transfer the rf signal into the photonic carrier wave from a constant laser diode. The light was coupled into and out of the 4-bit TTD device through single-mode fibers and was finally fed into a high-speed detector. The rf signal from the photodetector was amplified and fed into the network analyzer. With the rf frequency scanning, the relative phase would change at a fixed rate, which was determined by the time delay of the device. However, each scanning line was not a perfect straight line, with some deviation caused by environmental noise or system cross talk. If we subtract the linear fitted baseline value from each measured phase change, phase error can be obtained, which represents the rf signal quality. The measured data values oscillate rapidly within 4° due to environmental

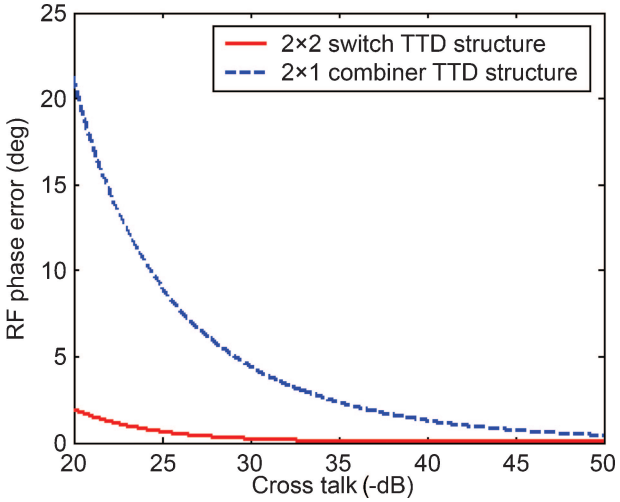

Fig. 6. (Color online) Simulated rf phase error caused by the optical switch cross talk.

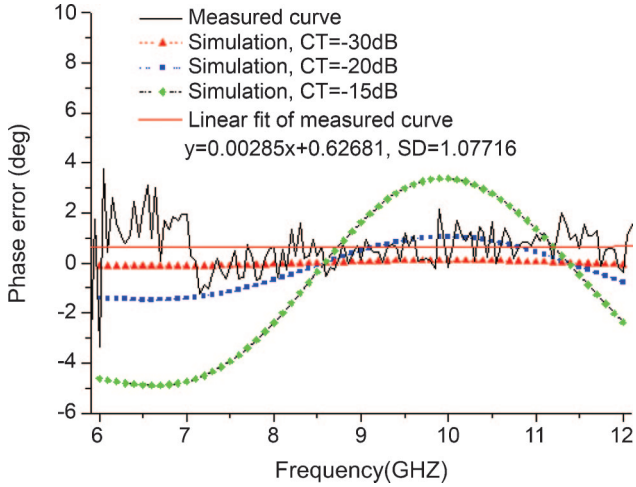

Fig. 7. (Color online) Simulation and experimental results of the rf phase error.

noise. The linear fitted curve has a standard deviation of 1.08° and a slope of 0.00285°/GHz, corresponding to a -7.9 fs measurement error. Simulated phase error curves with different cross-talk values, however, show gradual baseline variation, which is different from the measured result. The standard deviation of the measured phase and delay error in all 16 working states are also presented in Table 1. A conclusion can be drawn that the rf phase error caused by optical switch cross talk is negligible for the device, compared with environmental noises.

4. Summary

The fabricated 4-bit polymer TTD device using fully integrated TIR switches exhibits accurate delays, low power consumption, small chip size, and low fabrication costs. The switching time of the TIR switches is below 3 ms. Simulations predict that the cross-talk-induced rf signal phase error is negligible. This result is confirmed by the experimental data.

This research is supported by the Navy Space and Naval Warfare Systems Command and the Air Force Office of Scientific Research.

References

1. W. Ng, A. Walston, L. Tangonan, J. J. Lee, I. Newberg, and N. Bernstein, "The first demonstration of an optically steered microwave phased array antenna using true-time-delay," J. Lightwave Technol. **9,** 1124–1131 (1991).
2. Z. Shi, Y. Jiang, B. Howley, Y. Chen, F. Zhao, and R. T. Chen, "Continuously delay-time tunable-waveguide hologram module for x-band phased-array antenna," IEEE Photon. Technol. Lett. **15,** 972–974 (2003).
3. K. Horikawa, I. Ogawa, H. Ogawa, and T. Kitoh, "Photonic switched true time delay beam forming network integrated on silica waveguide circuits," IEEE MTT-S Int. Microwave Symp. Dig. **1,** 65–68 (1995).
4. J. D. Shin, B. S. Lee, and B. G. Kim, "Optical true time-delay feeder for X-band phased array antennas composed of 2×2 optical MEMS switches and fiber delay lines," IEEE Photon. Technol. Lett. **16,** 1364–1365 (2004).
5. B. Howley, Y. Chen, X. Wang, and R. T. Chen, "2-bit recon-

figurable true time delay lines using 2×2 polymer waveguide switches," IEEE Photon. Technol. Lett. **17,** 1944–1946 (2005).
6. Q. Lai, W. Hunziker, and H. Melchior, "Low-power compact 2×2 thermooptic silica-on-silicon waveguide switch with fast response," IEEE Photon. Technol. Lett. **10,** 681–683 (1998).
7. H. Kogelnik and R. V. Schmidt, "Switched directional couplers with alternating $\Delta\beta$," IEEE J. Quantum Electron. **12,** 396–401 (1976).
8. X. Wang, B. Howley, M. Y. Chen, and R. T. Chen, "Crosstalk minimized polymeric 2×2 optical switch," IEEE Photon. Technol. Lett. **11,** 16–18 (2006).
9. Y. O. Noh, J. M. Kim, M. S. Yang, H. J. Choi, H. J. Lee, Y. H. Won, and S. G. Han, "Thermo-optic 2×2 asymmetric digital optical switches with zero-voltage operation state," IEEE Photon. Technol. Lett. **16,** 446–448 (2004).
10. X. Wang, B. Howley, M. Y. Chen, and R. T. Chen, "Polarization-independent all-wave polymer based TIR thermo-optic switch," J. Lightwave Technol. **24,** 1558–1565 (2006).
11. A. A. Szep, "Polymer-based integrated optical waveguide true time delay for wide-band phased array antennas," Ph.D. dissertation (University of Southern California, 2002), pp. 17, 22–36.
12. G. L. Tan, R. E. Mihailovich, J. B. Hacker, J. F. DeNatale, and G. M. Rebeiz, "Low-loss 2- and 4-bit TTD MEMS phase shifters based on SP4T switches," IEEE Trans. Microwave Theory Tech. **51,** 297–304 (2003).